The coating sublimation process for annular plates forming a doubly connected slot channel (in planform) is not self-similar and it is impossible to write a simple formula of the type (24) or (21) to compute the sublimation time. However, even in this case the kinetics can be computed comparatively simply by numerical methods since the internal and external phase transformation fronts also remain circles here that move oppositely to each other until they meet, which means completion of the process. For instance, a sufficiently simple algorithm can be proposed that will reduce to a step-by-step process of the following kind: we separate the domain $\xi'' < \xi < \xi'$ having the coating into N annular layers $\xi_n < \xi < \xi_{n+1}$, $\xi_n = \xi'' + (n/N)(\xi' - \xi'')$ and we calculate the change in coating thickness at the middle of each annular layer by formulas similar to (19), i.e., for $\xi = \xi_{n1} = {}^1/_2(\xi_n + \xi_{n+1})$ the functions $\delta(\xi_{n1}, t)$ are calculated. After the coating thickness has become zero, at the middle of one of the external annular layers, the appropriate front is displaced one step into the domain under consideration, i.e., continuous phase transformation front motion is here replaced by a stepwise process. It is natural to expect that the error in determining the coating sublimation time by such a numerical method will tend to zero as $N \to \infty$.

NOTATION

H and L, height and linear scale of the flow in the middle plane of a slot channel, respectively; λ, mean free path length of the molecules; $\varepsilon = H/L$; T, local temperature; $\tau = (T - T_0)/T_0$; n, numerical molecule density; $n_{\ell w}(T_w)$, equilibrium value of the numerical molecule density at the wall temperature T_w (on the saturation line); $\nu = (n - n_0)/n_0$; β, condensation coefficient; R, universal gas constant; m, molecule mass; $\bar{u}$, velocity; t, time; $Q_v^{(0)}(\alpha)$, dimensionless velocity (flow rate) averaged over the channel height; $\alpha = \sqrt{\pi}H/3\lambda$; j_m, vapor mass density from the channel wall; ξ, η, dimensionless rectangular coordinates in the middle plane of the channel, referred to the channel height; and Kn, Knudsen number. Subscripts: w, on the wall; and 0, at the point $\bar{r}_0$.

LITERATURE CITED

1. P. A. Novikov and L. Ya. Lyubin, Inzh.-Fiz. Zh., 51, No. 6, 985-990 (1986).
2. D. A. Labuntsov, Teplofiz. Vys. Temp., 5, No. 4, 647-654 (1967).
3. H. Schlichting, Boundary Layer Theory, McGraw-Hill (1960).

OXYGEN-FREE VAPOR CONVERSION OF METHANE

A. M. Dubinin, A. P. Baskakov,
O. M. Panov, and B. L. Choinzonov

UDC 66.071:669.046

A reactor for the purpose of methane conversion is described. Comparison of a calculation of a mathematical model of the device with experimental data shows good agreement.

At the present time methane conversion is the basic industrial method for production of technological gases used to extract iron from ores by the direct reduction method. Tube furnaces used for this purpose require a large amount of expensive special fire-resistant steel, while mine reactors generate expensive gas due to their use of oxygen.

The reactor with a retarded fluidized bed described in [1] is free of these shortcomings. A diagram of this device is shown in Fig. 1. The retort 14 is packed with a catalyst 5, in the pores of which a fine grain material which acts as an intermediate heat-exchange agent circulates. In the "boiling" layer of these particles above the packing 7 a tuyere consisting of tube 9, "sleeve" 10, and perforations 8 is immersed.

S. M. Kirov Ural Polytechnic Institute, Sverdlovsk.

Translated from Inzhenerno-Fizicheskii Zhurnal, Vol. 52, No. 1, pp. 80-86, January, 1987. Original article submitted November 15, 1985.

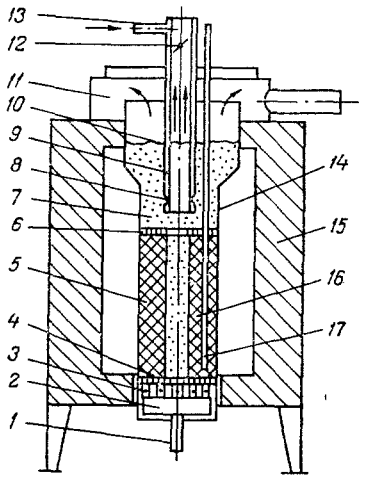

Fig. 1. Diagram of experimental reactor: 1) vapor–gas mixture supply; 2) gas distribution chamber; 3) domes; 4) lattice; 5) catalytic packing; 6) lattice; 7) fluidized bed; 8) perforations; 9) inner tube; 10) "sleeve"; 11) collection chamber; 12) gate valve; 13) air supply; 14) retort; 15) thermal insulation; 16) standpipe; 17) thermocouple casing.

Superheated water vapor mixed with methane is supplied through gas distribution lattice 2. A portion (x) of the conversion products formed in the catalyst by the endothermal reaction

$$CH_4 + H_2O = CO + 3H_2 \quad (1)$$

is removed through tube 9 for end use.

The heat required for reaction (1), heating of the products, and compensation of thermal losses is produced by burning of the remainder of the products (1 − x) in the annular gap between the retort 14 and the tuyere and transferred into the volume of the packing by the particles of finely dispersed material.

The air required for the resulting exothermal reaction

$$CH_4 + H_2O + 2(O_2 + 3{,}76N_2) = CO_2 + 3H_2O + 7{,}52N_2 \quad (2)$$

is supplied through "sleeve" 10 and passes into the layer through perforations 8. The combustion products are removed from the reactor through chamber 11.

For complete mixing of the finely dispersed particles over the retort section the steady-state problem of temperature and methane concentration distribution in the catalytic packing can be considered one-dimensional and described by the following system of ordinary nonlinear differential equations in ordinary derivatives:

$$\lambda \frac{d^2t}{dz^2} = q_{c_1} s \varepsilon k \rho_m r_m P + m G_{c.p} c_{c.p} \frac{dt}{dz}; \quad (3)$$

$$-\frac{G_{c.p}}{\rho_{c.p}\varepsilon} \frac{dr_m}{dz} = k s r_m P; \quad (4)$$

$$k = 87{,}5 \exp[-E/(R(t+273))]; \quad (5)$$

$$\rho_m = \rho_{m,n.c} \frac{273}{t+273}; \quad (6)$$

$$\rho_{c.p} = \rho_{c.p,n.c} \frac{273}{t+273}(1+2r_m). \quad (7)$$

Boundary conditions:

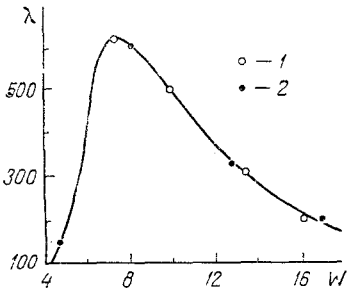

Fig. 2

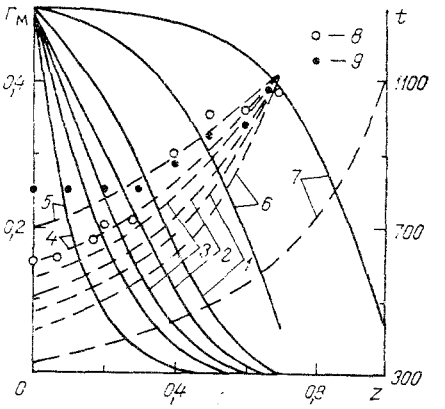

Fig. 3

Fig. 2. Vertical component of thermal conductivity coefficient of retarded fluidized bed λ (W/(m·K)) vs fluidization number W: 1) d = 0.32; 2) 0.42 mm.

Fig. 3. Distribution of temperature t (°C) and methane concentration over catalytic packing height z (m); calculation: 1) λ = 400, 2) 500, 3) 600, 4) 700, 5) 1000 W/(m·K), $G_{c.p}$ = 0.06 kg/(m²·sec), H = 0.7 m; 6) λ = 600 W/(m·K), $G_{c.p}$ = 0.15 kg/(m²·sec), H = 0.7 m; 7) experimental-industrial reactor λ = 600 W/(m²·K), $G_{c.p}$ = 0.2 kg/(m²·sec), H = 1 m; experiment: $G_{c.p}$ = 0.06 kg/(m²·sec), H = 0.7 m; 8) without standpipe; 9) with standpipe; solid lines, r_m; dashes, t.

at z = 0

$$r_m = r_{m,o}; \tag{8}$$

$$\lambda \frac{dt}{dz}\bigg|_{z=0} + mG_{c.p}(q_m + q_v) = mG_{c.p}c_{c.p}t_{z=0}; \tag{9}$$

at z = H

$$[q_{c_2}(1 - q_3 - q_5) + q_a](1 - x) + q_m + q_v = q_{c1}x\left(1 - \frac{r_{m,f}}{r_{m,o}}\right) + [c_{com}(1 - x) + c_{c.p}v]t_{z=H}. \tag{10}$$

The left side of Eq. (3) expresses heat transport due to the vertical component of the effective thermal conductivity of the fluidized bed of finely dispersed particles, while the right side describes heat expenditure to internal drains (the endothermal methane reaction, Eq. (1)) and heating of the conversion products in the elementary layer of catalytic packing. The reactions in the equations for methane concentration are of first order.

Equation (4) represents the balance between the convective influx of reacting methane mass and loss of this mass due to chemical conversions. Because of its smallness as compared to the convective influx, the diffusion flow of mass can as usual be neglected.

Equation (5) defines the rate constant of reaction (1), i.e., the methane volume flow rate relative to methane partial pressure (at atmospheric mixture pressure and the temperature in the layer) for the methane reacted per unit catalyst surface.

Equations (6) and (7) consider the dependence of the density of natural gas and the conversion products on temperature, with the latter equation also considering their dependence on the volume fraction of methane they contain.

The boundary condition at the input to the packing (z = 0) is a thermal balance equation for the heat supplied from the fine grained material, the natural gas, and the vapor and the heat expended in heating the conversion products, Eq. (9). We neglect dependence of specific heat on mixture composition and temperature. The volume fraction of methane in the vapor–gas mixture is equal to its original value, Eq. (8).

At the output from the packing (z = H) boundary condition (10) expresses equality of the heat liberated in burning the fraction of the methane (1 − x) which enters the reactor (with consideration of incomplete chemical reaction and heat loss into the surrounding medium) and the heat supplied from the air, natural gas and vapor on the left side, to the heat ex-

TABLE 1. Composition of Reducing Gas

Regime	Dry gas, vol.%			
	CO_2	H_2	CH_4	CO
1 (without standpipe)	1,27	78,64	0,81	19,28
2 (with standpipe)	0,86	79,72	0,25	19,17

TABLE 2. Composition of Combustion Products

Regime	Dry gas, vol.%				Incompleteness of combustion, %
	CO_2	O_2	N_2	CO	
1 (without standpipe)	8,01	2,06	89,3	0,62	1,92
2 (with standpipe)	9,32	2,66	87,89	0,13	0,7

pended in the endothermal reactions and removed from the reactor with the combustion and conversion products on the right side.

At the beginning of the calculations $r_{m,f}$ was chosen and the degree of methane conversion calculated and substituted in Eq. (10). The temperature and concentration fields were then calculated. The value of $r_{m,f}$ obtained was compared to that chosen beforehand. When the two values did not agree, one half their sum was chosen as a new initial value. When the preselected and calculated values coincided (within the limits of computation accuracy) the iteration process was halted.

All quantities appearing in Eqs. (3)-(10) are referenced to 1 kg of methane introduced into the reactor.

The calculations used values of volume fraction of methane in the original vapor–gas mixture $r_{m,o} = 0.5$, reactor pressure P = 0.1 MPa, activation energy E = 65.5 MJ/mole, heat introduced into the reactor by water vapor $q_v = 551$, by methane $q_m = 44$, by air $q_a = 391$ kJ/kg methane, specific heat loss to incomplete reaction $q_3 = 0.15$, the loss to the surroundings $q_5 = 0.1$, specific catalyst surface $s = 258$ m^2/m^3, and porosity $\varepsilon = 0.345$. Thermal calculations yielded the value $x = 0.25$.

The value of the effective heat-transport coefficient of the finely dispersed particles λ in the direction opposite the motion of the gas flow was taken from data shown in Fig. 2 of [2]. The dependence of the quantity λ on fluidization number W was obtained from the layer energy equation by comparing the experimental temperature field to the calculated one. Measurements were performed in a fluidized bed retarded by packing, with air draft and retort walls electrically heated to 850°C.

From an analysis of calculations of temperature and methane concentration fields in the catalytic packing, performed on an SM-4 computer, it is evident that efficiency of operation of such a reactor depends to a significant degree on the heat transport coefficient λ (Fig. 3). The greater the value of λ the higher the mean temperature, and hence, the reaction rate (curves 1-5). Increase in mass velocity of the conversion products $G_{c.p}$ has a converse effect on temperature and concentration distributions (curves 3 and 6).

The modeling performed indicated the possibility of practical realization of such reactors. Therefore, experiments were performed with an OKB-724A endogenerator with 180-mm-diameter retort, rebuilt according to Fig. 1. Synthetic corundum particles with d = 0.32 mm were used as the intermediate heat-transfer agent. They circulated in a packing H = 0.7 m high, formed of cylindrical particles of KSN-2 catalyst with grain size 15 × 15 mm. The inner diameter of the tube for conversion product removal was 82 mm.

Tests of the reactor for a conversion product mass velocity of $G_{c.p} = 0.06$ kg/(m^2·sec) showed that the composition of the gas obtained (Table 1) satisfied the requirements of a reducing atmosphere. The temperature distribution over height of the catalytic packing corresponded qualitatively and quantitatively to that predicted by the mathematical model (Fig. 3, curve 8).

In order to increase the intensity of heat transfer by the particles in the catalyst volume, a standpipe 16 (Fig. 1), 52 mm in diameter, was placed in the center of the chamber, with the aid of which a directed flow of the dispersed material was created at a rate of 1 kg/sec (26 kg corundum per 1 kg reducing gas). Since the hydraulic resistance of the packing with dispersed material is less than the head created by the continuous column of material

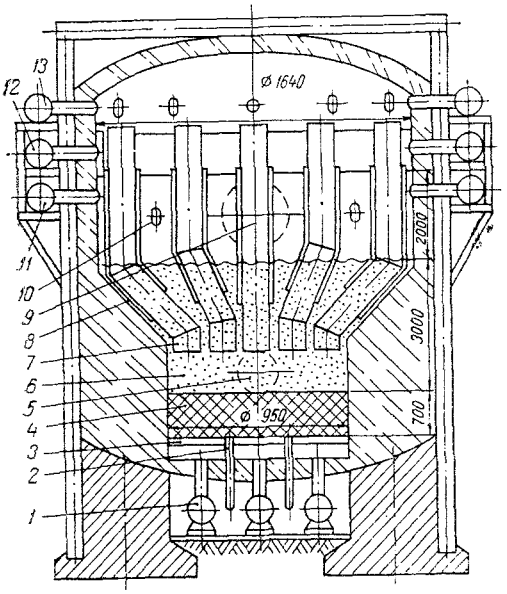

Fig. 4. Experimental-industrial reactor: 1) vapor and methane supply; 2) corundum drain; 3) gas distribution lattice; 4) catalytic packing; 5) manhole; 6) fluidized bed; 7) tuyeres; 8) air supply channels; 9) blast valve; 10) corundum filler; 11) combustion product exhaust; 12) air supply; 13) conversion product exhaust.

TABLE 3. Basic Parameters of Experimental-Industrial Reactor

Parameter	Value
Reducing gas output, 10^3 m^3/h	0,5
Pressure, MPa:	
vapor–methane mixture	0,25
air	0,3
Product temp., °C	
conversion	950
combustion	950
Methane content, %:	
converted	42,5
burned	57,5
Flow rates:	
methane, 10^3 m^3/h	0,294
water vapor, ton/h	0,236
air, 10^3 m^3/h	1,85
Combustion product output, 10^3 m^3/h	2,19
Efficiency, %	27,9

in the standpipe, the material moves upward in the packing volume and down through the standpipe. Thus, the temperature of the gas at the entrance to the packing could be increased by almost 200°C (Fig. 3, curve 9).

Gas analysis showed that the standpipe had no effect on the composition of the conversion products, i.e., untreated gas does not pass through the standpipe (Table 1, regime 2).

The composition of the gas leaving the burnup zone is shown in Table 2. Incompleteness of combustion here varied from 0.7 to 1.92%, depending solely on the excess air coefficient. The experimental results showed that burnup does not pollute the reducing atmosphere produced.

On the basis of these studies, following a coordinated plan of scientific-research studies and introduction of their results into practice in 1985-1986, as supported by the Ministry of Ferrous Metallurgy of the USSR, a task force was created for design of a self-heated experimental-industrial reactor for conversion of methane by water vapor with production of 500 m^3/h for the Oskol electrometallurgical plant.

In the calculations performed, following the data of [2] (Fig. 2), the value of λ was chosen close to the maximum (λ = 570 W/(m·K)). The number W was used to determine the mass

flow of conversion products $G_{c.p}$. To increase the latter the diameter of the circulating corundum particles was chosen equal to 0.5 mm. The mathematical model allowed using the temperature and methane concentration distributions within the reactor (Fig. 3, curve 7) to obtain the required height of the catalytic packing (H = 1 m).

The construction of the reactor designed is shown in Fig. 4, while its basic operating parameters are presented in Table 3. After construction designs were developed, the reactor was converted from operation with water vapor to use for conversion of methane gas when fed by the circulation gas exiting from a furnace used for reduction fo iron ore nodules (composition: CH_4, 3.0; CO, 20.1; CO_2, 17.2; H_2, 42.0; H_2O, 14.2; N_2, 3.5%). Such reactors can be used to replace low reliability tube furnaces which require large expenditures of imported high alloy steel and catalyst.

NOTATION

c, mean mass specific heat at constant pressure per 1 kg methane supplied to the reactor, J/(kg·K); d, particle diameter, mm; E, activation energy, J/mol; G, mass flow rate, kg/(m²·sec); H, catalytic packing height, m; k, chemical reaction rate constant, m/sec; m, quantity of methane required for production of 1 kg of conversion product, kg; P, pressure, atm; q_{c1}, q_{c2}, heats of chemical reactions (1) and (2), J/kg of natural gas; q_3, q_5, heat losses for incomplete combustion and to surroundings; q, heat, J/kg of natural gas; R, universal gas constant, J/(mol·K); r, volume content of methane; s, specific surface of catalytic packing, m^2/m^3; t, temperature, °C; W, fluidization number; x, fraction of conversion product removed from reactor; z, vertical coordinate, m (measured from lower face of catalytic packing toward upper); ρ, density, kg/m^3; ε, packing porosity; λ, effective heat transfer coefficient, W/(m·K). Subscripts: a, air; o, original; f, final; m, methane; n.c, normal conditions; v, vapor; c.p, conversion products; com, combustion products.

LITERATURE CITED

1. A. M. Dubinin, A. P. Baskakov, and V. B. Shoibonov, Inventor's Certificate No. 992079, "Endothermal atmosphere generator," Byull. Izobret., No. 4 (1983).
2. A. P. Baskakov, B. V. Berg, A. F. Ryzhkov, and N. F. Filippovskii, Heat and Mass Transport Processes in a Fluidized Bed [in Russian], Moscow (1978).

STRIKING DYNAMICS AND ENERGY CHARACTERISTICS OF A BULK DISCHARGE WITH UV PREIONIZATION NEAR THE THRESHOLD VOLTAGE

V. N. Karnyushin, P. P. Samtsov, and R. I. Soloukhin

UDC 621.375

Measurements have been made on the effects of preionization on the striking and energy characteristics of a bulk discharge near the threshold voltage.

Considerable use is made of UV preionization in pulsed laser systems, which has stimulated numerous studies on the ionization and energy characteristics [1-3]. A necessary condition for obtaining a bulk discharge (BD) at pressures of about 1 atm is the production of an initial electron density n_0 of about 10^6-10^8 cm^{-3} in the gap, while the electrodes subsequently receive a voltage pulse whose amplitude U_0 exceeds some threshold value U_1 slightly dependent on n_0 [4, 5].

There is interest in the striking dynamics and energy characteristics of BD for U_0 close to U_1 primarily because then the ratio of the electric field E to the gas pressure P lies closest to the value optimal for pumping CO_2 laser levels [2]. The highest efficiency is

Lykov Institute of Heat and Mass Transfer, Academy of Sciences of the Belorussian SSR, Minsk.

Translated from Inzhenerno-Fizicheskii Zhurnal, Vol. 52, No. 1, pp. 86-89, January, 1987. Original article submitted September 17, 1985.

0022-0841/87/5201-0068$12.50